



Development of textile nanocomposites with thermal energy storage capability

Emel Onder^{1,a} & Nihal Sarier²

¹ Faculty of Textile Technologies and Design, Istanbul Technical University, Gumussuyu Campus, 34437 Taksim, Istanbul, Turkey

² Faculty of Engineering, Istanbul Kultur University, Atakoy Campus, 34158 Bakirkoy, Istanbul, Turkey

Received 20 July 2020; revised received and accepted 20 November 2020

In this study, textile-based composites with dynamic heat storage capability have been designed and developed, in addition to their existing passive insulation capacity. First, poly(acrylonitrile) (PAN) shell and poly(ethylene glycol) (PEG1000 or PEG1500) cores are produced by coaxial electrospinning. Then, these are incorporated into felt based composite structures, which demonstrate enhanced thermal properties as well as buffering function against temperature changes in the environment. The thermal energy absorption and release capacities of the felt composites including PAN-PEG1000 or PAN-PEG1500 nanowebs are measured as high as 81 Jg^{-1} between $33 \text{ }^\circ\text{C}$ and $46 \text{ }^\circ\text{C}$, and 48 Jg^{-1} between $46 \text{ }^\circ\text{C}$ and $54 \text{ }^\circ\text{C}$ respectively. Felt composites, combined with PAN-PEG nanowebs offer forthcoming production applications in the field of dynamic thermal management in various industries.

Keywords: Differential scanning calorimetry, Dynamic mechanical analysis, Electrospinning, Nanocomposite, Phase change materials, Poly(acrylonitrile), Poly(ethylene glycol), Thermal camera images

1 Introduction

In recent years, breakthroughs in the production of electrospun nanofibres, especially in their applications in the energy and environmental sectors, have opened the possibility of ensuring sustainable energy and preserve environment for the future^{1,2}. Thermal energy storage using phase-change materials (PCMs) is one of the effective methods of conserving energy due to their high-energy storage densities and small temperature variations from storage to retrieval². The number of studies dealing with new PCM applications have shown considerable increase in recent years, to seek new solutions and to develop new products in context of thermal energy utilization in many different areas. Among them, the use of solid-liquid organic PCMs have been offering great potential for the thermal management applications across various industries such as solar energy storage³, buildings⁴, textiles⁵, and thermal protection⁶. They have the ability to absorb and release large amounts of latent heat during melting and solidification processes, possessing both thermal and chemical stabilities against multiple thermal cycles over a long period, thereby creating a buffer effect against temperature changes.

Before integrating into different composites, a variety of encapsulation and storage methods has been applied to PCMs, with the goal of preventing their interaction with the surrounding medium, thus increasing their mechanical and thermal stabilities and enhancing their ease of handling^{2,6}. Coaxial electrospinning as a new electrospinning technique for the production of shell-core nanofibres has been receiving more and more attention lately^{7,8}. Through coaxial electrospinning, PCMs can be encapsulated in a polymer shell. The nanofibres consisted of a PCM core and a polymer shell possess remarkable advantages, such as to avoid the leakage of PCM during phase change processes, to form a large surface area with the numerous nanofibres, to be lightweight, and to hold good mechanical strength. Therefore, they can be directly used in various composites^{9,10,11}. Since the type of PCMs plays a dominant role on the morphology and thermal properties of electrospun polymer-PCM composite fibres, many innovative types of PCMs have been used to fabricate novel PCM fibres.

The preparation, properties and applications of heat-storage textiles and clothing have been extensively studied for more than thirty years. At present, their fabrication involves in integration of microencapsulated PCMs or melt-spun / electrospun polymer fibers with various PCMs to fabrics and foams, or direct coating of the surface with PCM and

^aCorresponding author.
E-mail: onderem@itu.edu.tr

binder mixtures. However, these applications have some disadvantages that limit the textile applications of PCMs, such as increased weight and thickness of the fabrics, decrease in their flexibility, durability, breathability and thermal conductivity^{2,12}.

To the best of our knowledge, there has been no attempt for the use of PCM nanowebs supported by nonwoven textile surfaces, which can then be incorporated within the ceiling and floor tiles of buildings, the interior trim of automobiles and airplanes, or can be used as the cover of temperature sensitive packages. In our previous study, we produced the poly(acrylonitrile) (PAN) shell and poly(ethylene glycol) (PEG1000 or PEG1500) core nanowebs (NWs) and characterized those NWs with respect to the structure, morphology, thermal properties, and stability¹⁰. This study focuses on the design and development of the textile-based nanocomposites integrated with PAN-PEG NWs, which have the capability of dynamic heat-storage in addition to the existing passive insulation characteristic of the structure. With this aim, we produced PAN-PEG NWs by coaxial electrospinning as thermal energy storage (TES) materials. The thermal and mechanical properties of these nanowebs as well as their structural characteristics were examined in detail. Then, we incorporated PAN-PEG NWs between two felt layers (felt layer: bonding layer: PAN-PEG NW: bonding layer: felt layer), and finally developed two sandwich-like structures. These structures were then characterized for their thermal and thermo regulating properties.

2 Materials and Methods

2.1 Materials

Poly (acrylonitrile) (PAN) was chosen as the shell material for the coaxial electrospinning process, owing to its non-reactivity with the core material as well as its ultra-fine fibre forming properties, high mechanical and thermal performances and high moisture management properties. PAN copolymer, consisting of 99.5% acrylonitrile (AN) and 0.5% maleic anhydride (MAH), $(\text{H}_2\text{CHCN})_n$ ($MW_{av}150,000 \text{ gmole}^{-1}$, density 1.18 gcm^{-3}) was supplied from Good Fellow Corp. (Catalog Num: AN316010/748-840-78) in powder form.

Poly(ethylene glycols) (PEGs) with the molecular weights of 1000 gmole^{-1} (PEG1000) and 1500 gmole^{-1} (PEG1500) were used as the core materials, owing to their capability for repeatable solid-liquid phase changes at low and moderate temperature intervals,

their high heat of fusions (ΔH_{fus}) as well as their chemical and thermal stability, non-toxicity and low price^{2,6}. PEG1000, PEG1500 and the chemical reagent dimethyl acetamide (DMAc, $\text{C}_4\text{H}_9\text{NO}$) were purchased from Sigma-Aldrich Inc. All were of technical grade and used without further purification in the coaxial electrospinning process.

For the manufacture of sandwich-like structures, a nonwoven textile sheet made from 100% polyester felt, weighing 100 gm^{-2} and suitable for thermal insulation applications, was kindly supplied from Hassan Textile A.Ş. (Istanbul, Turkey) and a 50.50 polyamide-polyester lining (L) weighing 36 gm^{-2} , suitable for the fixation of partial textile surfaces in the production of fine and soft-handling apparel, was kindly supplied from Telasis Industry and Trade Inc. (Istanbul, Turkey).

2.2 Methods

2.2.1 Coaxial Electrospinning of PAN-PCM Nanofibres

Recently, our research group reported the production of PAN nanofibres encapsulating PEGs and PEG derivatives as novel thermal energy storage materials¹⁰. To inspect temperature regulation efficiency of the bicomponent PAN (shell) and PEG (core) nanowebs in textile-based composites, PAN-PEG1000 and PAN-PEG1500 NWs, were reproduced via coaxial electrospinning for two hours, using the electrospinning device Yflow Co. (Spain)^{10,13}. The spinneret of the device consists of two stainless steel coaxial needles with outer diameters (ODs) of 0.9 /1.7 mm and inner diameters (IDs) of 0.6 /1.4 mm respectively, connected to a reservoir. The grounded flat stainless-steel plate was placed 15 cm from the coaxial nozzles, and a double polarized system (30 kV, +30 kV) was used to effectively collect the nanowebs. The process parameters for coaxial electrospinning were finely tuned to ensure compound Taylor cone formation for each of the specimens. Table 1 shows the optimized coaxial electrospinning parameters for the production of PAN-PEG NWs.

PAN solution of 6 wt% in DMAc was prepared in a glass flask at a stirring rate of 500 rpm at 35 – 40 °C. The core solutions of 40 wt% PEG 1000 or PEG 1500 were prepared in DMAc solvent at 25 °C.

2.2.2 Preparation and Characterization of Composite Enclosing PAN-PEG Nanowebs

The process of incorporating PAN-PEG NWs into textile composites was carried out on a laboratory-type LaStar lining machine, available in the research laboratory of Telasis Textile Products Industry and

Table 1 — Optimized coaxial electrospinning parameters for the production of PAN-PEG nanoweb [Duration 2 h]

Sample code	Shell (in DMAc)	Core (in DMAc)	Shell pump rate, mLh ⁻¹	Core pump rate, mLh ⁻¹	Injector voltage kV	Collector voltage kV
PAN (Control)	6% PAN	-	0.03	-	7.0	-7.0
PAN-PEG1000	6% PAN	40%PEG1000	0.10	0.08	8.0	-8.0
PAN-PEG1500	6% PAN	40%PEG1500	0.10	0.08	8.0	-8.0

Table 2 — Sizes, masses and surface densities of felt composites

Composite code	Type of NW	Size of sample cm × cm	Total mass, g	Mass of NW layer in sample, g	Surface density gm ⁻²
D (Control)	-	21.0 × 14.0	6.08	0.00	206.8
D1	PAN-PEG1000	20.5 × 14.5	9.37	6.94	315.2
D2	PAN-PEG1500	20.8 × 15.0	9.28	3.06	297.4

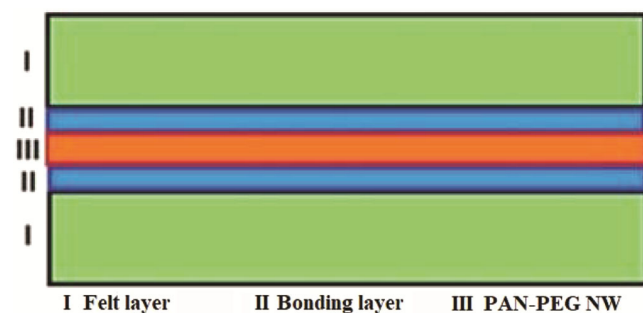


Fig. 1 — Scheme of PAN-PEG NW incorporated felt-based nanocomposites

Trade Inc. (Istanbul, Turkey). A sandwich-like composite structure, composed of the outer felt layer (I), adhesive interlining sheet (II) and PAN-PEG nanoweb sheet (III) (Fig. 1), was passed through a rotating couple of the lining machine under the pressure of 2.5 bar at 132 °C for 24 s for fixation, and then immediately removed. The properties of the felt based nanocomposites are summarized in Table 2.

2.3 Analytical Methods

Morphologies of the NW specimens were examined via scanning electron microscopy (SEM) using an EVO® LS 10 model Zeiss type SEM (LaB6-Tungsten filament) at 5–10 kV. From the SEM images with 15.00 K magnification, the diameter distributions of nanofibres were computed via the Image J-Diameter J software for 100 nanofibres on average¹².

Thermogravimetric analyses (TGA) of the NWs were performed from 20 °C to 800 °C at a 10 °Cmin⁻¹ heating rate under a dry nitrogen atmosphere purged at the rate of 20 mLmin⁻¹ by a SEIKO EXSTAR 6200 Model TG/DTA instrument.

The tensile behavior of the PAN-PEG NWs was analyzed on Mettler Toledo Dynamic Mechanical Analyzer (DMA SDTA861) by using the large tensile module of a 19 mm gauge length. The test specimens,

which had the dimensions of 19.500 mm length, 5.000 mm width and 0.100 mm thickness (geometry factor 39.000 x 10³ m⁻¹), were subjected to tensile forces varying in a range of 0.1– 1.0 N by a moveable clamp of the DMA tension module at 1 Hz frequency and at the room temperature (25°C). The results were obtained in terms of elastic/storage modulus and the loss factor.

Thermal properties of the NW samples and textile composites were examined by a Perkin Elmer DSC 4000 Differential Scanning Calorimeter (DSC) with an accuracy of ±0.001. A nitrogen flux (20 mLmin⁻¹) was used as a purge gas for the furnace. Temperature scans were run on samples that were placed in a closed pan and that weighed 10 – 15 mg for ten successive heating and cooling cycles.

For examining actual thermal responses of the nanoweb, Infra-red (IR) thermal camera images of NWs were taken by FLIR T640 model IR Thermal Imaging Camera (FLIR Systems, Inc., USA) with the resolution of 640 x 680 and magnification capacity of x 8. Prior to the thermal camera image taking, the NW samples (PAN-PEG1000 and PAN-PEG1500) as well as the felt composite samples (D1 and D2) and D (Control) were kept at 60 °C in an oven for 10 min, then they were set on the glass plate and their IR images were taken in 30 s intervals for 10 min. When the specimens reached thermal equilibrium with the surroundings, they were immediately placed over the ice block(-10 °C) and then the IR image taking was continued for further 5 min.

3 Results and Discussion

3.1 SEM Images and Fibre Diameter Distributions of PAN-PEG NWs

The SEM images as well as the fibre diameter distributions of the PAN-PEG1000 and PAN-PEG1500 NWs are shown in Fig. 2. The SEM images

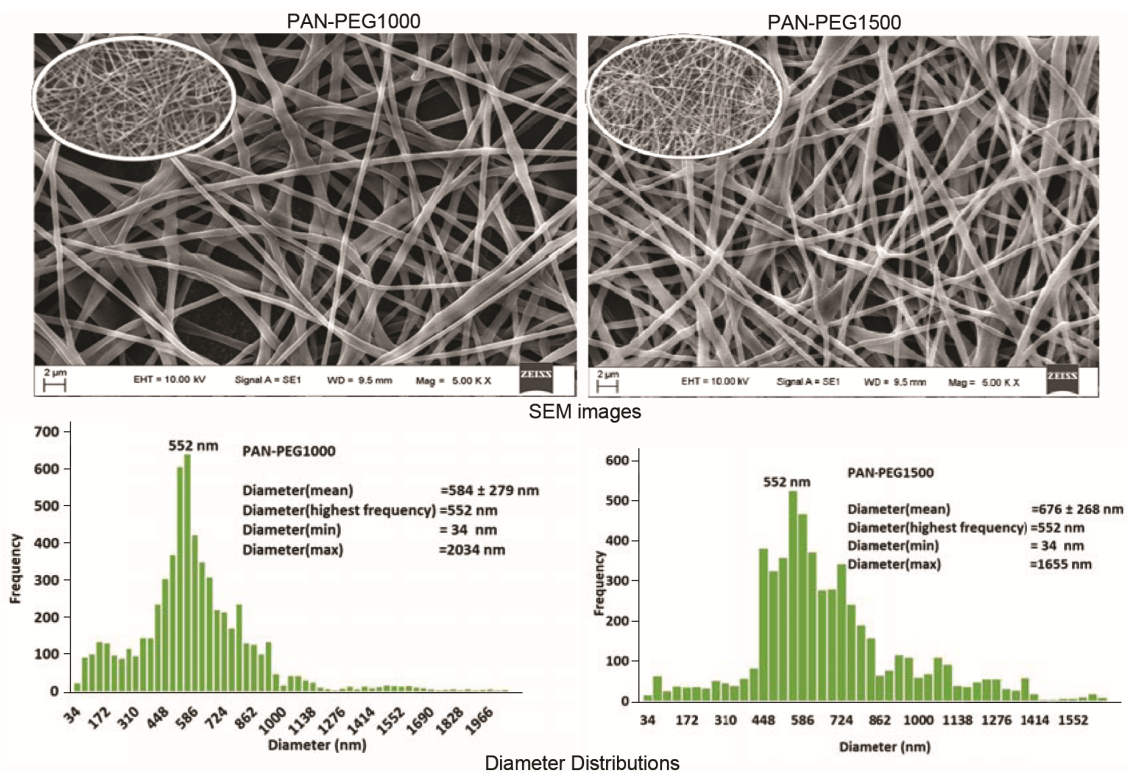


Fig. 2 — SEM images [$\times 5.00$ K magnification (inset $\times 2.00$ K)], and diameter distributions of PAN-PEG1000 and PAN-PEG1500 (obtained from SEM image with $\times 5$ K)

display cylindrical, beads, smooth surface and long nanofibres that are distributed randomly and densely through each image. The PEG chains are not noticed outside each of the PAN-PEG NW SEM images, indicative of the successful encapsulation of PEG1000 and PEG1500 in a PAN shell under given electrospinning conditions.

According to the diameter analysis results, 90% of the fibre diameters in the SEM images of PAN-PEG1000 and PAN-PEG1500 are found at the sub-micron scale. Although the nanofibres seemed to have wider cross-sections in some parts, the highest frequency for the diameters of both is 552 nm. On the other hand, the percentage of nanofibres having a diameter less than or equal to 500 nm is 44% for PAN-PEG 1000 and 28% for PAN-PEG 1500. The mean nanofibre diameters are calculated as 584 ± 281 nm (PAN-PEG 1000) and 676 ± 268 nm (PAN-PEG 1500). The fineness of PAN-PEG NWs indicates that they could easily be incorporated into textile composite structures¹⁰.

3.2 TGA Results of PAN-PEG NWs

TGA data of PAN-PEG NWs, obtained in our previous study¹⁰, are represented in Fig. 3. The thermal decompositions of PAN-PEG1000 and PAN-PEG1500 nanowebs started to accelerate at about 270–285 °C

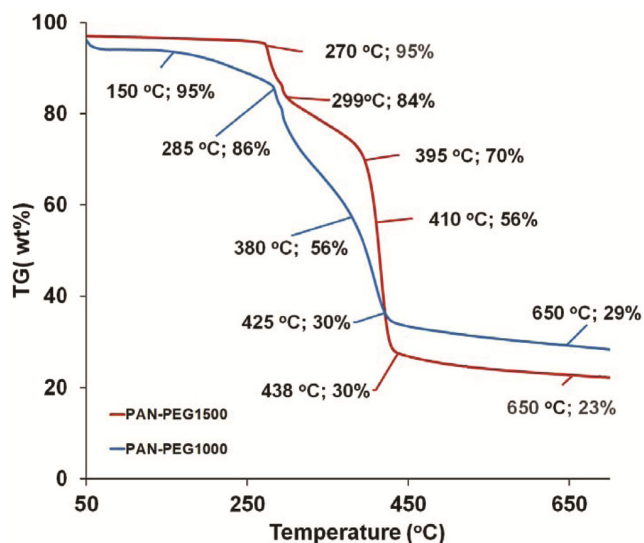


Fig. 3 — TGA curves of PAN-PEG1000 and PAN-PEG1500 nanowebs¹⁰

and finalized at 650 °C with 23 – 29 % residue. These findings show that PAN-PEG NWs are thermally stable; therefore, they are suitable for the preparation of a composite in the coating machine at 132 °C and can be used in heat management applications under ordinary ambient conditions.

3.3 Dynamic Mechanical Analysis (DMA) Tensile Test Results of PAN-PEG NWs

Dynamic mechanical analysis is a useful technique to measure the mechanical responses of a material to stress, strain, temperature, frequency and other factors studied when a small sinusoidal deformation is applied to a sample. DMA measurements are reported as the storage modulus (E'), the loss modulus (E''), and the damping factor ($\tan \delta$). The storage modulus (E') is the measure of the sample's elastic behavior and stiffness; and the loss modulus (E'') is the measure of its viscous response. The ratio of the loss modulus to the storage modulus (E''/E') is the damping factor ($\tan \delta$), which is the measure of ability of a material to dissipate mechanical energy in the form of heat, useful in understanding internal motions of the polymer chains¹⁴.

The variation of storage modulus (E'), loss modulus (E''), and damping factor ($\tan \delta$) of PAN (Control), PAN-PEG1000 and PAN-PEG1500 NWs with respect to the applied tensile force (0.1–1.0 N) at 25 °C are given in Table 3. When E' and $\tan \delta$ data of PAN-PEG1000 and PAN-PEG1500 NWs are compared with those of PAN (Control), it is observed that the presence of PEG cores within PAN-PEG NWs does not weaken the mechanical properties of PAN, which is in good agreement with the data reported before in the literature for PAN including nanofibres¹⁵. Therefore, they can easily be subjected to elastic deformations and sustain considerable

tensile forces which implies their suitability for use as a functional sheet in textile composites.

Storage modulus (E') values of PAN-PEG1000 and PAN-PEG1500 NWs exhibit steady increase compared to that of pristine PAN (Control) owing to the molecular orientation of PAN and PEG chains¹⁶, indicating improvement of their stiffness when subjected to tensile forces. In the case of PAN-PEG1500 NW, the storage modulus of the sample drops suddenly to 0.02 MPa when the tensile force approaches to 0.5 N due to the restricted mobility of the longer chains of PEG1500 compared with PEG1000¹⁶. The damping factor ($\tan \delta$) values of PAN-PEG1000 NW (5.74×10^{-2} – 6.49×10^{-2}) are slightly lower than those of PAN (Control) (5.09×10^{-2} – 8.11×10^{-2}), which can be attributed to the interfacial interactions between PAN and PEG chains in PAN-PEG1000 NW. On the other hand, the $\tan \delta$ of PAN-PEG1500 NW is slightly higher than that of PAN (Control) due to the restricted mobility of PEG1500 chains as mentioned above. The loss modulus values (E'') of PAN-PEG1000 NW ($E''_{\text{mean}} = 17$ MPa) and PAN (Control) ($E''_{\text{mean}} = 18$ MPa) are found in the same range and also increase to some extent as the tensile force applied increases, whereas E'' values of PAN-PEG1500 are found slightly higher, suggesting gradual loss of its mechanical resiliency.

3.4 DSC Results of PAN-PEG NWs and Felt Composites

DSC data of PEG1000, PEG1500 and of the PAN-PEG NW samples, obtained from 10th DSC heating-cooling cycles, are given in Table 4. The phase

Table 3 — DMA tensile test results of the NWs in terms of storage modulus (E'), loss modulus (E''), and damping factor ($\tan \delta$) at 25 °C

Time, s	Force, N	PAN (Control)			PAN-PEG1000			PAN-PEG1500		
		E' MPa	E'' MPa	$\tan \delta$ $\times 10^{-2}$	E' MPa	E'' MPa	$\tan \delta \times 10^{-2}$	E' MPa	E'' MPa	$\tan \delta$ $\times 10^{-2}$
1	0.1	170.90	8.70	5.09	184.34	10.58	5.74	246.35	17.24	7.00
20	0.2	193.09	11.73	6.07	208.05	15.17	7.29	295.77	27.84	9.41
39	0.3	203.10	12.86	6.33	219.23	14.66	6.69	333.90	35.08	10.51
59	0.4	212.69	13.56	6.37	267.22	16.68	6.24	355.07	44.05	12.41
78	0.5	261.06	17.16	6.57	288.20	17.71	6.14	0.02	0.00	0.00
99	0.6	274.84	18.95	6.90	303.40	18.41	6.07	0.00	0.00	0.00
111	0.7	281.00	19.64	6.99	312.50	19.01	6.08	0.00	0.00	0.00
126	0.8	284.94	20.59	7.23	318.41	19.68	6.18	0.00	0.00	0.00
141	0.9	289.28	23.16	8.01	323.78	20.55	6.35	0.00	0.00	0.00
153	1.0	290.13	23.54	8.11	328.64	21.31	6.49	0.00	0.00	0.00

Table 4 — Thermal behavior of PEG1000, PAN-PEG1000, PEG1500 and PAN-PEG1500 during 10th heating and cooling cycles of DSC analysis

Sample	10 th Heating			ΔH Jg ⁻¹	10 th Cooling			ΔH Jg ⁻¹
	T_{onset} , °C	T_{peak} , °C	T_{end} , °C		T_{onset} , °C	T_{peak} , °C	T_{end} , °C	
PEG1000	31	39	41	158	28	22	14	158
PAN-PEG1000	30	39	40	109	28	24	20	103
PEG1500	43	51	54	172	25	21	15	175
PAN-PEG1500	43	50	52	147	35	28	24	143

change enthalpy of PAN-PEG1000 NW is found 109.4 Jg^{-1} between $31 \text{ }^\circ\text{C}$ and $40 \text{ }^\circ\text{C}$ and that of PAN-PEG1500 NW is 146.6 Jg^{-1} between $43 \text{ }^\circ\text{C}$ and $52 \text{ }^\circ\text{C}$ during 10th heating cycle. The phase change enthalpies of PAN-PEG nanoweb specimens are remarkable regarding both concentrations and enthalpies of the cores used in electrospinning process, as evidence of successful formation of bicomponent nanofibres.

Figure 4 exhibits the DSC heating and cooling curves of D1 (including PAN-PEG1000 layer) and D2 (including PAN-PEG1500 layer). DSC curves in the 2nd and 10th heating-cooling cycles of D1 and D2 coincide essentially with the DSC curves of the nanoweb they contained. During heating cycle, the phase transition onset and end temperatures of D1 and D2 are shifted slightly to higher temperatures than the corresponding PEG and PAN-PEG nanofibre. This may be due to unstable heat transfer conditions in the felt composites. The phase change enthalpies of D1 and D2 felt composites are measured as 81 Jg^{-1} between $33 \text{ }^\circ\text{C}$ and $46 \text{ }^\circ\text{C}$, 48 Jg^{-1} between $46 \text{ }^\circ\text{C}$ and $54 \text{ }^\circ\text{C}$ during 10th heating cycle, respectively. There is no significant change in heat capacities and phase transition temperature ranges in ten heating and cooling cycles in

each sample. These findings indicate thermal cycling stability of the produced composite structures, and there is no leakage in the structure. Consequently, we can say that the dynamic thermal insulation of these felt composites has been achieved successfully by incorporating the PAN-PEG layer into the structure.

3.5 Thermal Camera Images of Nanoweb and Felt Composites

The surface temperatures of PAN-PEG1000, PAN-PEG1500 nanoweb and felt composites (D2 and D) obtained from the IR images as a function of time are given in Fig. 5, 6 and 7 respectively, to observe their thermal energy release and temperature regulation efficiency against ambient temperature changes. In IR images, light colored regions indicate areas with higher temperatures; dark spots indicate low temperature zones. The time-dependent temperature variation data obtained from the IR images of PAN-PEG1000, PAN-PEG1500 and D2 are consistent with the data of DSC measurements.

As seen in Figs 5 and 6, after drawing out the nanoweb specimens from the oven, the initial temperatures of PAN-PEG1000 and PAN-PEG1500 are $42.7 \text{ }^\circ\text{C}$ and $53.8 \text{ }^\circ\text{C}$ at 10th s respectively, while

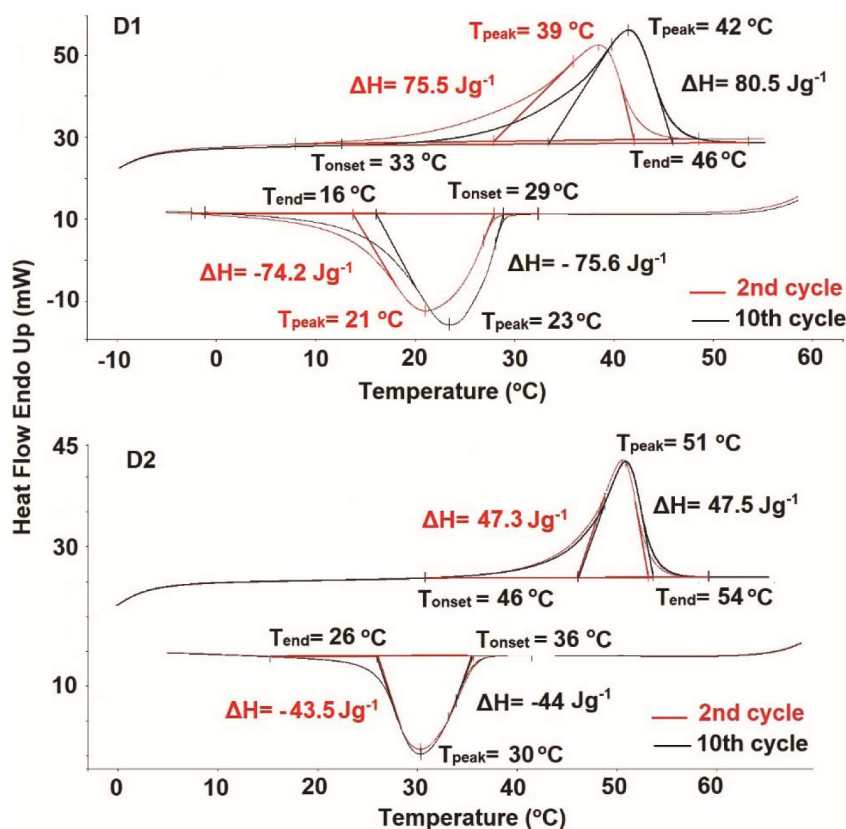


Fig. 4 — DSC 2nd and 10th heating and cooling curves for D1 (PAN-PEG1000) and D2 (PAN-PEG1500)

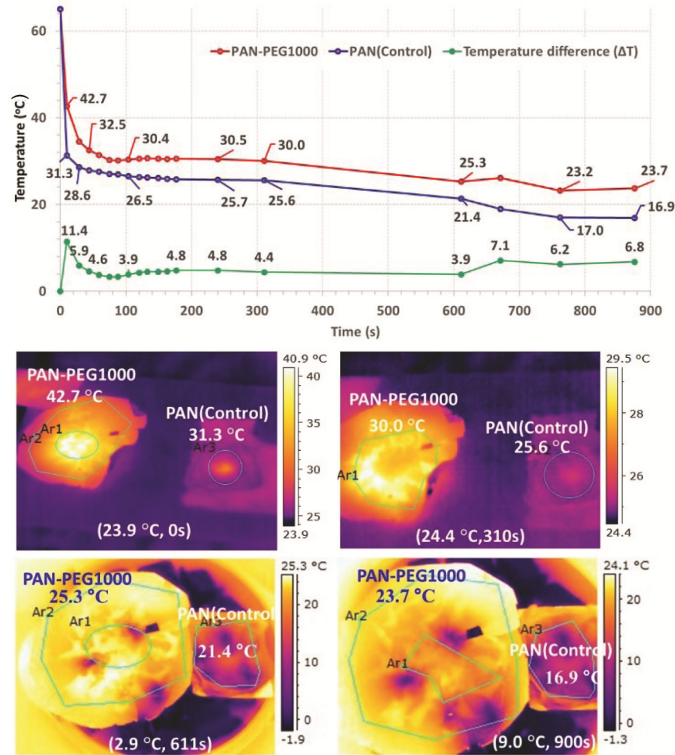


Fig. 5 — Temperature versus time graphs, obtained from the thermal camera measurements for PAN-PEG1000 with respect to PAN (Control), and thermal camera images of PAN-PEG1000 (Ar2) and PAN(Control) (Ar3) taken at different times

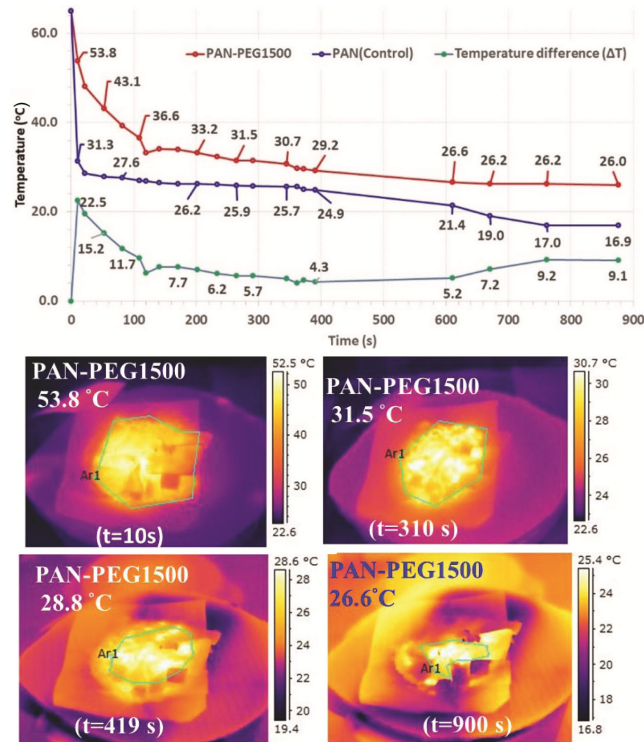


Fig. 6 —Temperature versus time graphs, obtained from the thermal camera measurements for PAN-PEG1500 with respect to PAN (Control), and thermal camera images of PAN-PEG1500 (Ar1) taken at different times

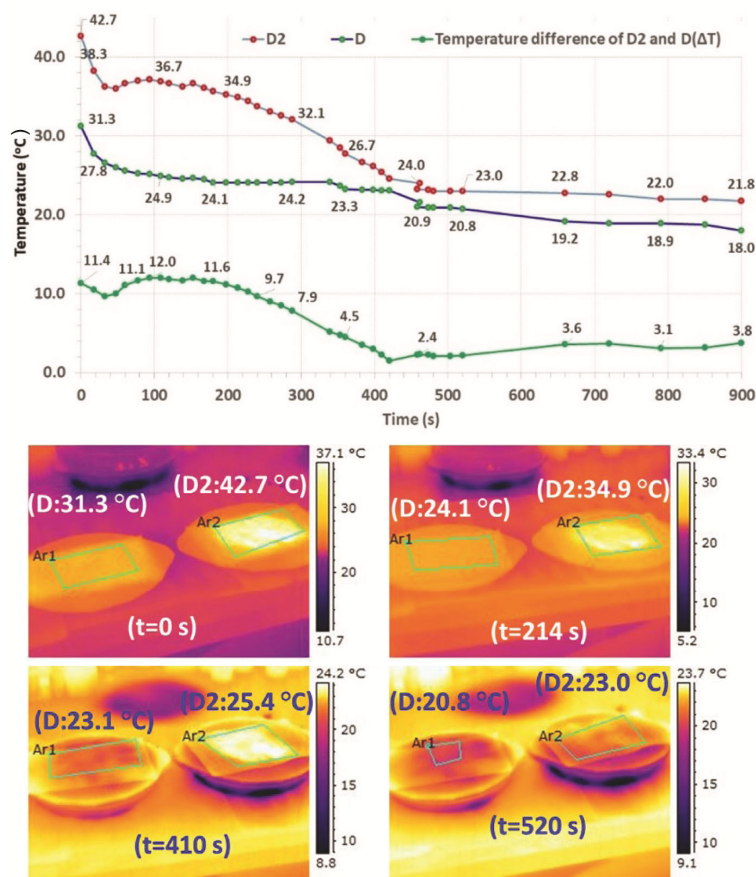


Fig.7 — Temperature versus time graphs, obtained from the thermal camera measurements for D2 with respect to D (Control), and thermal camera images of D2 (Ar2, right) and D (Control) (Ar1, left) taken at different times

that of PAN (Control) drops instantly to 31.3 °C. Then, the surface temperatures of PAN-PEG1000 and PAN-PEG1500 gradually decrease, as compared to PAN (Control). For example, at 310th s, the temperatures of PAN-PEG1000 and PAN-PEG1500 reduce to only 30.0 °C and 31.5 °C, while the temperature of PAN (Control) drops to 25.6 °C. After 900 s, over the ice block, the surface temperatures of the PAN-PEG1000 and PAN-PEG1500 are 23.0 °C and 26.0 °C, while the temperature of PAN (Control) drops to 16 °C. These findings show that the temperature regulation efficiency of PAN-PEG nanoweb to ambient temperature changes are quite successful¹⁷.

As shown in Fig. 7, after drawing out D2 (including PAN-PEG1500) and D (Control) from the oven at 60.0 °C, the initial temperature of D2 is measured as 42.7 °C at 10th s, while that of D (Control) drops instantly to 31.3 °C. As time passes, the temperature difference between D2 and D (Control) increases. At the 310th s of the measurements, D (Control) attains room temperature (24.0 °C), while the

temperature of D2 decreases to only 34.8 °C. After placing both of the samples on ice block at 410th s, the temperature of D2 drops to 25.4 °C and that of D (Control) to 23.1 °C. When the phase transition process of PAN-PEG1500 NW [Fig. 4 and Fig. 7] is over (after 400 s), the surface temperature of D2 continued to be higher than that of D (Control) due to the heat stored through the layers of D2 sample. After 900 s, the temperature of D2 is 21.8 °C, while the temperature of D (Control) dropped to 18 °C. These results demonstrate that D2, enclosing PAN-PEG1500 nanoweb layer, has excellent thermal energy storage and dynamic temperature regulation performance in addition to passive thermal insulation capacity of the layered felt structure, in consistent with the literature^{18,19}.

4 Conclusion

In the present study, we designed and developed felt-based composites with dynamic heat storage capability, in addition to the existing passive insulation capacity of their structure. Distinctive

properties of PAN-PEG1000 and PAN-PEG1500 nanowebs, produced by coaxial electrospinning, can be listed as: high heat storage capacity, thermal stability, no leakage of the core, increased heat-transfer area owing to the nanofibre structure, good elastic deformation against tensile forces, and easy to apply to textile-based composites. The phase change enthalpies of the felt composites, including PAN-PEG 1000 and PAN-PEG 1500, are measured as 81 Jg^{-1} between $33 \text{ }^\circ\text{C}$ and $46 \text{ }^\circ\text{C}$ and 48 Jg^{-1} between $46 \text{ }^\circ\text{C}$ and $54 \text{ }^\circ\text{C}$ with DSC. The IR camera data demonstrated that the time-dependent thermal responses of PAN-PEG nanowebs and their felt composites to ambient temperature changes are quite successful.

In summary, the heat capacities, heat absorption-release temperature intervals, thermal stability and sealing properties of the felt nanocomposites, incorporated with PAN-PEG1000 or PAN-PEG1500 nanowebs, are found to be very suitable for applications in relevant temperature ranges. They are promising for further manufacturing practices in the area of thermal management across various industries including building or automobile ceiling, floor or other interior applications for thermal comfort and energy conservation purpose, temperature-controlled packaging of foods and medicines, biomedical materials for thermal therapy, thermal sensors, thermoelectric systems, apparels for cold and hot environments and solar energy systems.

Acknowledgement

Authors are thankful to the Scientific & Technological Research Council of Turkey (TUBITAK) for funding the project (213M281) to carry out this work. They also thank Telasis Textile Products Industry and Trade Inc. (Istanbul, Turkey) for their technical assistance.

References

- 1 Wang L, Chen C & Huang Y, Electrospinning of Phase-Change Materials for Thermal Energy Storage, in *Electrospun Nanofibers for Energy and Environmental Applications, Nanostructure Science and Technology*, edited by B Ding and J Yu (Springer: Heidelberg New York Dordrecht London), 2014, Chap. 9, 229.
- 2 Onder E & Sarier N, Thermal Regulation Finishes for Textiles, in *Functional Finishes for Textiles: Improving Comfort, Performance and Protection*, edited by R Paul (Elsevier: Amsterdam), 2015, Chap.1,17.
- 3 Shuangmao W & Guiyin F, *Energy Build*, 43(5) (2011) 1091.
- 4 Pasupathy A, Velraj R & Seeniraj R, *Renew Sust Energ Rev*, 12(1) (2008) 39.
- 5 Sarier N & Onder E, *Thermochim Acta*, 452 (2007) 149.
- 6 Sarier N & Onder E, *Thermochim Acta*, 540 (2012) 7.
- 7 Yarin AL, Zussman E, Wendorff JH & Greiner A, *J Mater Chem*, 17 (2007) 2585.
- 8 Yarin AL, *Polym Adv Technol*, 22 (2011) 310.
- 9 Lu Y, Xiao X, Zhan Y, Huan C, Qi S Cheng H & Xu G, *ACS Appl Mater Interfaces*, 10(15) (2018) 12759.
- 10 Noyan EC, Onder E, Sarier N & Arat R, *Thermochim Acta*, 662 (2018)135.
- 11 Dror Y, Salalha W, Avrahami R, Zussman E, Yarin AL, Dersch R, Greiner A & Wendorff JH, *Small*, 3 (2007)1064.
- 12 Shin Y, Dong-II Y & Kyunghye S, *J Appl Polym Sci*, 97(3) (2005) 910.
- 13 Yflow, Marie Curie 4–12, 29590 Campanillas, Malaga (Spain), 2019. <http://www.yflow.com/technology/coaxial-electrospinning/>; 2019 (accessed on 10.07.2019).
- 14 Duzyer S, Hockenberger A & Zussman E, *J Appl Polym Sci*, 120 (2011) 759
- 15 Mohammad N, Salman A & Chasiotis I, *Polymer*, 52 (2011) 1612.
- 16 Manoj N, Raut R, Sivaraman P, Ratna D & Chakraborty B, *J Appl Polym Sci*, 96 (2005) 1487.
- 17 Manral A & Bajpai PK, *Polym Comp*, 41 (2020) 691.
- 18 Lu X, Huang H, Zhang X, Lin P, Huang J, Sheng X, Zhang L & Qu JP, *Composites Part B: Eng*, 177 (2019) 107372.
- 19 Banerjee D, Chattopadhyay SK & Tuli S, *Indian J Fibre Text Res*, 38(4) (2013) 427.